Simulation Tools for Heavy-Ion Tracking and Collimation

P. D. Hermes, R. Bruce, F. Cerutti, A. Ferrari, J.M. Jowett, A. Lechner, A. Mereghetti, D. Mirarchi, P.G. Ortega, S. Redaelli, B. Salvachua, E. Skordis, G. Valentino, V. Vlachoudis
CERN, Geneva, Switzerland

Abstract
The LHC collimation system, which protects the LHC hardware from undesired beam loss, is less efficient with heavy-ion beams than with proton beams due to fragmentation into other nuclides inside the LHC collimators. Reliable simulation tools are required to estimate critical losses of particles scattered out of the collimation system which may quench the superconducting LHC magnets. Tracking simulations need to take into account the mass and charge of the tracked ions. Heavy-ions can be tracked as protons with ion-equivalent rigidity using proton tracking tools like SixTrack, as used in the simulation tool STIER. Alternatively, new tracking maps can be derived from a generalized accelerator Hamiltonian and implemented in SixTrack. This approach is used in the new tool heavy-ion SixTrack. When coupled to particle-matter interaction tools, they can be used to simulate the collimation efficiency with heavy-ion beams. Both simulation tools are presented and compared to measurements.

Keywords
Heavy-ions; ions; collimation; ion tracking; hiSixTrack; STIER

1 Introduction

The CERN Large Hadron Collider (LHC) [1] is a proton and heavy-ion collider reaching unprecedented beam intensities and particle momenta. In operation with $^{208}Pb^{82+}$ ions, the LHC has reached an integrated stored beam energy of 9.7 MJ, compared to only 3.6 MJ anticipated in the LHC design phase [1,2]. The destructive power of the stored $^{208}Pb^{82+}$ beams in 2016 is comparable to an explosion of more than 2 kg of TNT. Compared to that, the envisaged LHC upgrade to High Luminosity LHC (HL-LHC) [3] foresees another increase of the stored beam energy by a factor of two.

If large fractions of the stored beam energy are deposited in the LHC hardware, severe damage can be caused. But even tiny fractions of the stored beam energy are sufficient to induce magnet quenches (the transition from the superconducting to normal conducting state), which would reduce the time available for operation in stable beams. Compared to proton beams undesired losses and hence quench risk from heavy-ion collimation debris is significantly larger [4]. The origin for this observation is the fragmentation of heavy-ions into lighter ion fragments at their passage through the collimator.

The LHC collimation system [1, 5] has the task of intercepting undesired beam loss to protect the LHC hardware and avoid magnet quenches. Given the importance of collimation, it is indispensible to have reliable and accurate simulation software to anticipate the perfomance of the LHC collimation system with both proton and heavy-ion beams. Compared to tools for proton collimation simulations, heavy-ion simulation tools available before 2014 had a limited predictive power, due to different simplifications used in their physics models.

In this chapter, we indroduce the peculiarities related to the simulation of heavy-ion collimation. Based on these considerations two new simulation tools STIER and hiSixTrack available since 2014 and 2016 are presented. Typical applications are disucssed and an example analysis from the operation of the LHC with heavy-ion beams in 2015 is briefly summarized.

https://doi.org/10.23732/CYRCP-2018-002.73.

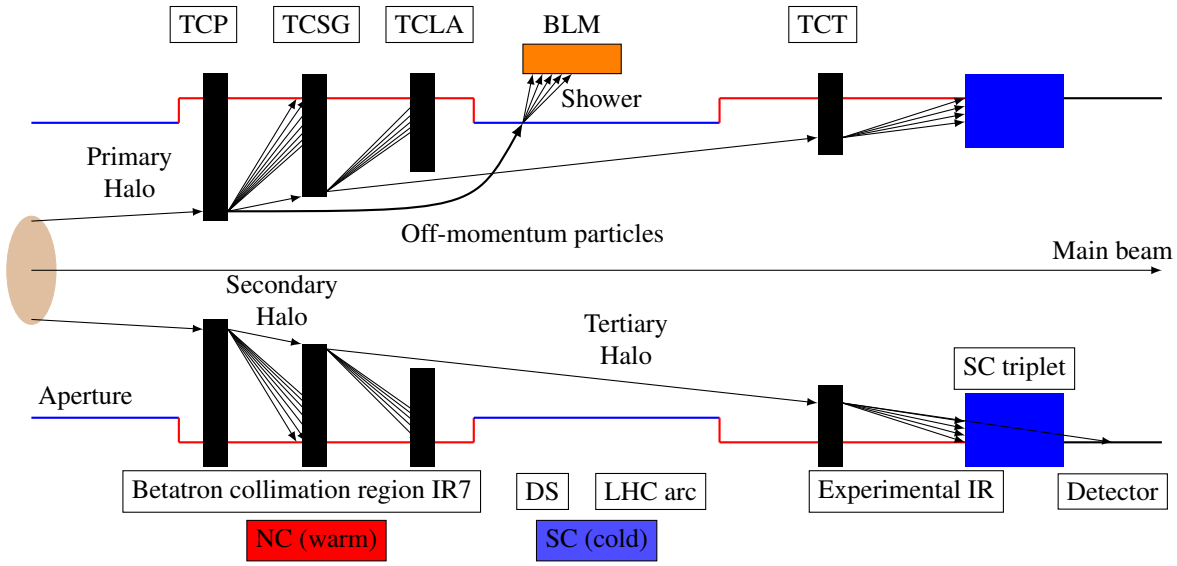

Fig. 1: Schematic overview of the LHC multi stage collimation system. Normal conducting (NC) regions are drawn in red, superconducting (SC) regions in red. Based on [6].

2 Collimation of Heavy-Ion Beams

2.1 The LHC Collimation System

2.1.1 Overview

To protect the LHC hardware from potential damage by undesired beam loss, the LHC is equipped with a multi-stage collimation system. One of the aims of the collimation system is to protect the superconducting LHC magnets from beam-induced magnet quenches, e.g. the transition from their superconducting to the normal conducting state. The latter would trigger an immediate beam dump and require several hours of cryogenic recovery, undesiredly reducing the LHC duty time for physics. The collimation system, illustrated for the betatron collimation region IR7 in Fig. 1 is designed for proton beams. It relies upon a defined sequence of collimation instances. Primary collimators (TCP) intercept beam particles at large transverse amplitudes. In the TCP, the beam particles shall be scattered into the secondary collimators (TCSG). Shower absorbers (TCLA) downstream of them provide protection from secondary hadronic and electromagnetic showers. Tertiary collimators (TCT) locally protect the superconducting triplets in the experimental insersions from particles scattered out of the secondary collimators.

In spite of the sophisticated collimation system with more than 100 collimators and the availability of many degrees of freedom to optimize the collimation performance, particles can still leave the collimation system and hit the superconducting LHC magnets. The superconducting magnets exposed to the highest amount of collimation losses, and hence under the highest quench risk, are those in the dispersion suppressor region (DS) downstream of IR7. The superconducting dipole magnets in this region act as a spectrometer on particles scattered out of the collimation system, which are not captured by the TCSG collimators. If particles have lost momentum compared to the main beam, or their mass and charge changed, their bending radius in the magnet will be different with respect to that of the reference particle. This effect leads to a transverse offset, ultimately resulting in a particle loss if the transverse offset exceeds the available beam pipe aperture in the magnet. To keep track of particle losses throughout the ring, the LHC is equipped with beam loss monitors (BLM) [7, 8] measuring secondary showers from particles interacting with the LHC hardware. The LHC beams can be transversally excited to induce losses at the collimation system and measure the cleaning inefficiency in a given machine configuration (qualification loss map) [9].

2.1.2 *Measurements of the Heavy-Ion Collimation Efficiency*

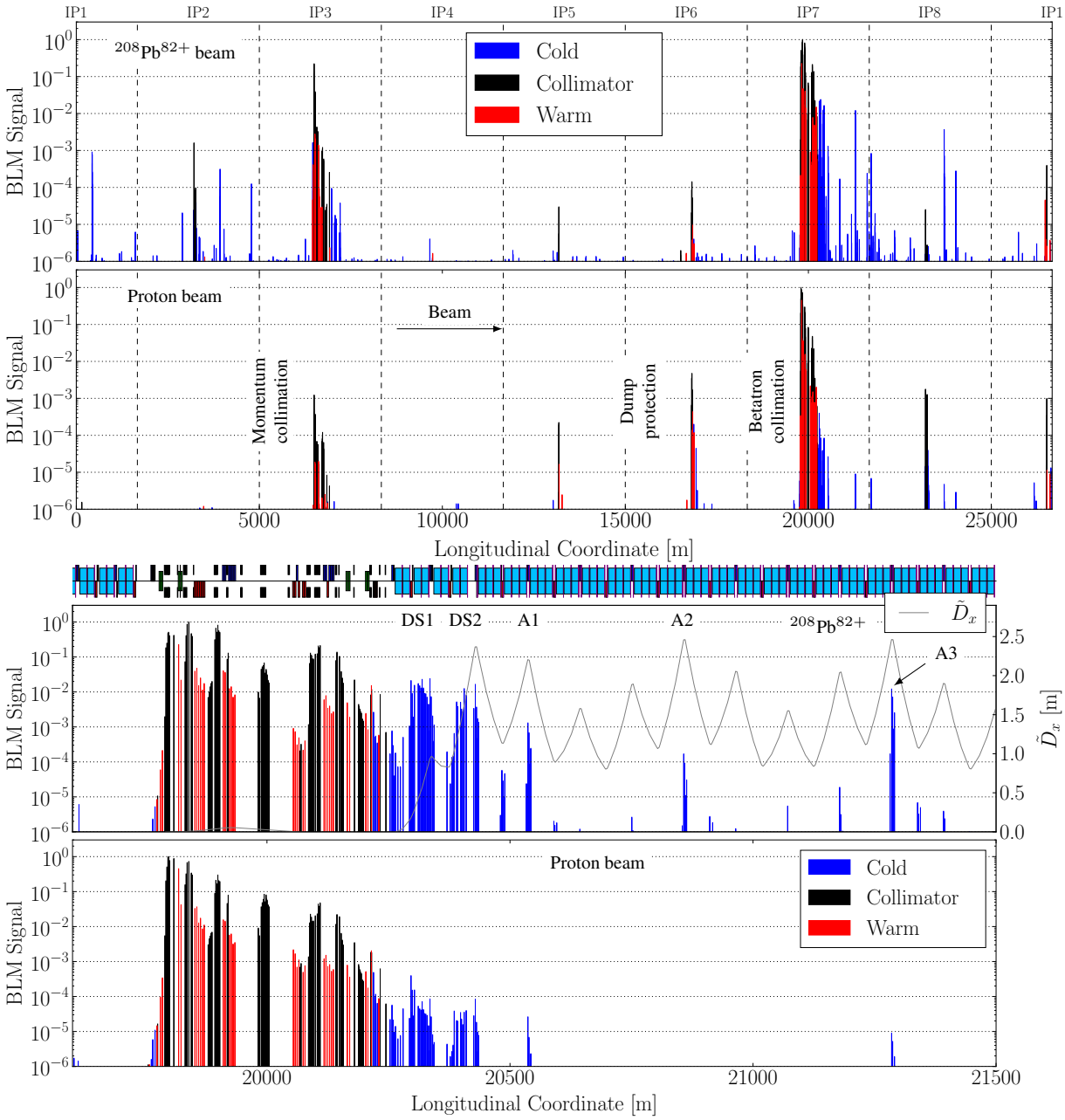

Fig. 2: B1H qualification loss maps measured in 2011 with proton [10] and $^{208}Pb^{82+}$ beams [11] at 3.5 Z TeV with identical collimator settings and optics, except in IR2. The longitudinal coordinate describes the distance from IP1. The vertical dashed lines mark the LHC octants. The BLM signals are normalized with respect to the highest measured BLM signal. Top: full LHC ring, bottom: zoom to IR7.

In Fig. 2, qualification loss maps for the horizontal plane of LHC beam 1 are compared for proton and heavy-ion beams at an energy of 3.5 Z TeV in 2011 (Z indicating the particle charge multiplicity) [12]. The BLM signal is always normalized with respect to the highest loss signal measured throughout the ring. The loss signals are color-coded to distinguish between losses in superconducting elements (blue), normal conducting elements (red) and losses at collimator (black).

In the upper plot in Fig. 2 it is clearly visible how the highest losses throughout the ring occur at the betatron collimation system in IR7 for both cases. For heavy-ion beams, also high losses in the

momentum collimation region IR3 are measured, which are smaller by two orders of magnitude for proton beams. Furthermore, the global picture illustrates that high loss peaks in superconducting LHC regions are visible for operation with $^{208}\mathrm{Pb}^{82+}$ ions all over the LHC ring. For proton operation, the losses in cold regions are localized closely to the collimators. The highest losses in cold regions are visible in the dispersion suppressor region immediately downstream of IR7 for both cases. However, the loss signal in heavy-ion operation is larger by approximately two orders of magnitude. Hence, the subject of heavy-ion collimation should be studied rigurously to ensure operation without beam induced magnet quenches.

The importance of heavy-ion collimation is furthermore underligned by the 2015 heavy-ion collimation quench test, in which the first beam induced magnet quench was achieved at the LHC [13]. In this experiment, high losses at the collimation system were provoqued and the particles scattered out of the collimators quenched the MBB.9R7 when a power load of $P_q = (15 \pm 1)\,\mathrm{kW}$ was deposited on the LHC collimators. The experimental data gathered in this experiment indicates that the beam intensity envisaged for HL-LHC may not be achievable with the present collimation system [4].

The theoretical understanding of losses from collimation inefficiency is crucial for the optimization and upgrade of the collimation system. Laborious simulations require to compute the particle motion through the accelerator lattice, simulate the interaction of the beam particles with collimators, follow the tracks of the out-scattered particles in the lattice and determine their loss location by comparing the tracks with the machine aperture. It is hence required to combine accurate particle tracking simulations with particle-matter interaction simulations and exchange information between them. From the comparison of measured loss maps it becomes clear that the collimation of proton and heavy-ion beams are fundamentally different, which must necessarily reflect in the simulation software. This applies especially to the losses in the IR7 DS region, which are induced by particles of an unmatched rigidity scattered out of the collimators. The keystone in the understanding of this difference lies in the interactions protons and heavy-ions can undergo in the collimators.

2.2 Particle Matter-Interaction in Collimators

Heavy-ions are composed of multiple protons an neutrons. The nuclide used in the LHC heavy-ion runs so far is $^{208}\mathrm{Pb}^{82+}$, with 208 nucleons in total. At the passage through the collimator, the heavy ions can interact with the atoms of the collimator material which can lead to scattering, energy loss and fragmentation. The type of interaction that is undergone is statistically dependent on the projected distance b of the heavy-ion (projectile) from the nucleus of the atom of the collimator material (target), the so called impact parameter (see Fig. 3). The most important effects in the theoretical description of heavy-ion-matter interaction are listed in the following.

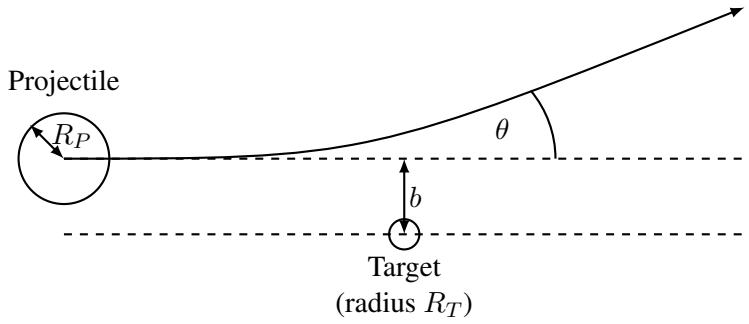

Fig. 3: Schematic illustration of the impact parameter.

2.2.1 Multiple Coulomb Scattering

Multiple Coulomb Scattering (MCS) is the repeated elastic scattering of the projectile due to the Coulomb interaction with the target nuclei. MCS leads to a broad spectrum of scattering angles when a projectile traverses the collimator. The mean scattering angle $\langle \Delta x'_{\mathrm{MCS}} \rangle$ can be described by the Molière formula, as presented in [14]. Given its independence of the particle mass and charge, the mean MCS angle is identical for protons and heavy-ions (see Tab. 1).

2.2.2 Energy Loss From Ionization

The traversing particles can ionize atoms of the target material, resulting in energy loss of the projectile. The mean energy loss from ionization per traversed distance in the material can be well quantified by the Bethe-Bloch formula [14]. The latter shows that the mean energy loss per length is quadratically proportional to the particle charge q.

2.2.3 Photonuclear Interactions

The charged projectile is surrounded by a Lorentz-contracted electromagnetic field which yields in a high photon flux between projectile and target nucleus. These photons can excite one or both of the nuclei into a higher energetic state. The nucleus deliberates from this excitated state preferably by the emission of one neutron. Generally, this type of photonuclear reation, referred to as electromagnetic dissociation (EMD) of the order m, can be summarized as [15]

$$\mathrm{EMD}m: \quad {}^{208}\mathrm{Pb}^{82+} + {}^{12}\mathrm{C} \rightarrow {}^{(208-m)}\mathrm{Pb}^{82+} + {}^{12}\mathrm{C} + m\,\mathrm{n}\,. \tag{1}$$

Photonuclear reations typically occur at ultraperipherical nuclear encounters, e.g. the sum of the nuclear radii is smaller than the impact parameter $b \geq R_P + R_T$. The most important process of EMD is the neutron emission of first order. For the reference species ${}^{208}\mathrm{Pb}^{82+}$ this corresponds to the dissociation into ${}^{207}\mathrm{Pb}^{82+}$. This isotope of Pb was shown to induce distinct losses in the LHC that can potentially impose a limitation on the achievable heavy-ion luminosity (see Sec. 5.2).

2.2.4 Nuclear Interactions

If the impact parameter is smaller than the sum of the radii of projectile and target nucleus, the particle can undergo nuclear interactions [16]. In these interactions the overlapping nuclei ablate parts of each other, resulting in nuclear fragmentation into a wide spred of different nuclei. Nuclear reations of ${}^{208}\mathrm{Pb}^{82+}$ with the carbon atoms of the collimator material can be summarized by the reaction formula

$${}^{208}\mathrm{Pb}^{82+} + {}^{12}\mathrm{C} \rightarrow {}^{A_X}\mathrm{X}^{Z_X+} + {}^{A_Y}\mathrm{Y}^{Z_Y+} + {}^{12}\mathrm{C} + N_n\,\mathrm{n} + N_p\,\mathrm{p} + ... \tag{2}$$

Here, X and Y are nuclides of a different species than ${}^{208}\mathrm{Pb}^{82+}$ whith their respective mass and charge numbers A_X, Z_X and A_Y, Z_Y. Furthermore N_n neutrons and N_p protons may be produced in the interaction. It is clear that also other particles, e.g. pions, electron, photons, etc. are produced in these interactions. They are neglegted in the framework of heavy-ion collimation software because the energy they carry is small compared to the heavy-ion fragments.

The most important nuclear interaction protons undergo with the nuclei of the collimator material is single diffractive scattering [17]. In this type of interaction, the proton is excited into a high mass state which desintegrates into a new proton and another particle. Evidently, the momentum of the created proton is reduced with respect to the incidenting one. This momentum offset is the cause for the subsequent particle loss in the DS if the scattering angle in the TCP is not sufficiently large to intercept the proton with the secondary collimators.

Table 1: Characteristic quantities for the most important physical processes of protons and lead ions traversing carbon-fiber composite (CFC) [1] at 7 Z TeV. Data taken from [20] and scaled to the density of CFC.

Physics Process	Unit	Proton	$^{208}\mathrm{Pb}^{82+}$
$-\frac{dE}{E\,\mathrm{d}x}$	$[10^{-5}\,\mathrm{m}^{-1}]$	11	917
$\langle\Delta x'_{\mathrm{MCS}}\rangle$	$[\,\mu\mathrm{rad}/\sqrt{m}]$	4.0	4.0
$\lambda_{\mathrm{nuclear}}$	[cm]	47.9	3.1
λ_{EMD}	[cm]	-	23.9

2.2.5 Nuclear Evaporation and Statistical Fragmentation

Heavy ions which have undergone a nuclear or photonuclear interaction are often in excited states. The ground state is reached by a variety of physical processes, including nuclear fission, nucleon emission or photon emission. The corresponding nuclear disintegration is referred to as nuclear evaporation [18]. Ion fragments of low masses may undergo statistical fragmentation, described by the Fermi breakup model [19].

2.2.6 Summary

The key parameters quantifying the aforementioned interactions are listed in Tab. 1. The mean scattering angle from MCS is identical for protons and heavy ions. The mean energy loss per length unit is larger for heavy-ions by almost two orders of magnitude. The nuclear interaction length $\lambda_{\mathrm{nuclear}}$ is ten times smaller for $^{208}\mathrm{Pb}^{82+}$ than for protons. Significantly more particles with rigidity offsets are hence generated at the passage of $^{208}\mathrm{Pb}^{82+}$ through the collimator material.

3 The Physics behind Heavy-Ion Tracking

3.1 Sources of Dispersion

Let A, Z, m be the mass number, charge number and rest mass of the tracked nucleus, and A_0, Z_0, m_0 the corresponding quantities for the reference particle. The magnetic rigidity for the reference particle with momentum P_0, charge $q_0 = Z_0\, e$ in a magnetic field B is given as

$$B\,\rho_0 = \frac{P_0}{q_0}\,, \tag{3}$$

where ρ_0 is the bending radius of the particle trajectory in the magnetic field. A particle with different momentum P, mass m or charge q will be subject to dispersion which results in a different bending radius ρ. The dispersion can be quantified by considering the ratio of magnetic rigidities of the particle with respect to the reference particle:

$$\frac{\rho}{\rho_0} = \frac{P}{P_0}\,\frac{q_0}{q}\,. \tag{4}$$

If the particle is of the same species as the reference particle ($q = q_0$ and $m = m_0$), the bending radius is given as

$$\frac{\rho}{\rho_0} = \frac{P}{P_0} = \frac{\beta\gamma}{\beta_0\gamma_0} = (1 + \delta_M)\,, \tag{5}$$

where we used the equality $P = m\beta\gamma c$, relating the momentum with the rest mass, relativistic velocity $\beta = \frac{v}{c}$ and Lorentz factor $\gamma = \frac{1}{\sqrt{1-\beta^2}}$. The quantitiy δ_M describes the momentum offset of a particle with respect to the reference particle if it is of the same species as the latter (mono-nuclide scenario):

$$\delta_M = \frac{P - P_0}{P_0} = \frac{\beta\gamma - \beta_0\gamma_0}{\beta_0\gamma_0}\,. \tag{6}$$

If the particle is of a different species than the reference particle (multi-nuclide scenario), the ratio of bending radii becomes

$$\frac{\rho}{\rho_0} = \frac{m}{m_0}\,\frac{q_0}{q}\,\frac{\beta\gamma}{\beta_0\,\gamma_0} = \frac{1+\delta_P}{\chi}\,, \tag{7}$$

where δ_P and χ are defined as

$$\delta_P = \frac{\beta\gamma - \beta_0\gamma_0}{\beta_0\gamma_0} = \frac{P\,\frac{m_0}{m} - P_0}{P_0} \qquad \text{and} \qquad \chi = \frac{q}{q_0}\,\frac{m_0}{m}\,. \tag{8}$$

The quantity δ_P describes the ion's offset of the momentum per mass unit relative to the reference particle. The dispersion due to the different mass and charge is described by χ, which is the mass to charge ratio, relative to the reference particle. These independent quantities describe the dispersive offset in a given optical accelerator lattice.

3.2 Tracking Ions as Protons of Equivalent Rigiditiy

The comparison of Eq. (5) and (7) shows that the bending behaviour of an ion different from the reference species (described by χ and δ_P) is identical to that of an ion of the reference species, if the momentum offset of the latter is given by

$$\delta_M = \frac{1+\delta_P}{\chi} - 1\,. \tag{9}$$

Hence, tracking software designed for tracking mono-nuclide beams can be used also for multi-isotopic beams, if an *effective momentum* is applied to the particles of the referernce species. The most important tracking software for proton beams used at CERN is SixTrack [], providing an environment for symplectic proton tracking over a large number of turns. If an effective momentum P_{eff} to the protons is applied, the proton trajectory will be identical to the heavy-ion trajectory. Using Eq. (9), the effective proton momentum to simulate the motion of an arbitrary ion with (q,m) in a magnetic lattice matched to the reference ion with (q_0,m_0) can be deduced as:

$$P_{\text{eff}} = P_0\,\frac{1+\delta_P}{\chi} = \frac{P}{Z}\,. \tag{10}$$

This approach is used in the simulation tool STIER [12] (see Sec. 4.3).

3.3 Symplectic Tracking Maps from a Multi-Nuclide Accelerator Hamiltonian

Instead of using unphysical parameters in the tracking (effective proton momenta), a more generic approach of computing heavy-ion trajectories can be provided from a generalized mathematical formalism. Starting point for the description of symplectic multi-nuclide tracking is a generalized accelerator Hamiltonian. The latter should take into account that the tracked particle may have mass and charge different from the reference particle. The derivation of this Hamiltonian is explained in detail in [4, 22]. We refer to the reference frame shown in Fig. 4. The final shape of the generic accelerator Hamiltonian for

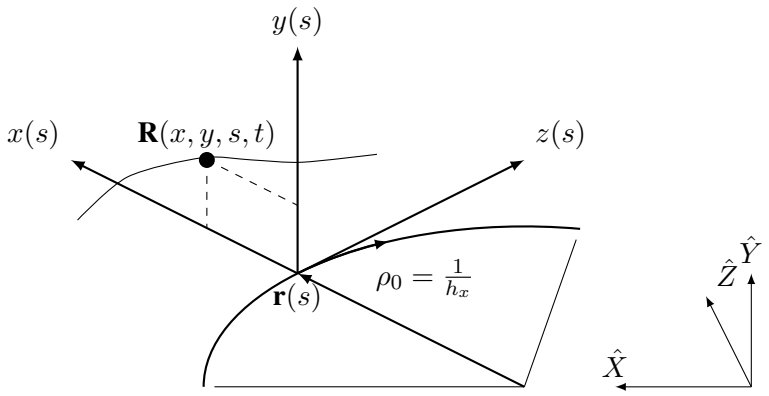

Fig. 4: Accelerator coordinate system (x, y, z) moving with $\mathbf{r}(s)$. The radius of the bent trajectory is $\rho_0 = \frac{1}{h_x}$. Figure taken from [21].

arbitrary particles with relative mass to charge ratio χ, momentum per mass offset $\delta = \delta_P$ moving in a magnetic field $\mathbf{B} = \nabla \times \mathbf{A}$ is given by

$$H = p_\sigma - (1 + h_x(s)\, x) \left(\sqrt{(1+\delta)^2 - (p_x - \chi a_x(s))^2 - (p_y - \chi a_y(s))^2} + \chi a_s(s) \right) . \tag{11}$$

The quantity $h_x = \frac{1}{\rho_0}$ is the curvature of the reference trajectory. The canonical coordinates associated to this Hamiltonian are

$$(x, p_x)\,(y, p_y)\,(\sigma, p_\sigma)\,, \tag{12}$$

with the longitudinal position coordinate σ and its canonical conjugate p_σ given as

$$\sigma = s - \beta_0\, c\, t\,, \qquad p_\sigma = \frac{\frac{m_0}{m}\, E - E_0}{\beta_0 P_0 c}\,. \tag{13}$$

Here, s is the longitudinal particle position, c is the speed of light, t the time and E, E_0 the energy of the particle and reference particle. Starting from this generic accelerator Hamiltonian, the tracking maps for the accelerator lattice elements can be derived, as discussed in [22].

4 Heavy-Ion Collimation Simulations

4.1 Introduction

Before discussing heavy-ion collimation tools we give a brief overview on the simulation of proton collimation. Proton collimation at the LHC the best studied scenario with the largest amount of measured data available to compare with the simulations. Furthermore, proton collimation is a special scenario of heavy-ion collimation (with an ion composed only of a proton), hence existing proton simulation tools can be upgraded for additional features making it possible to simulate heavy-ion collimation.

The present state of the art simulation tool for proton collimation simulations is SixTrack [17, 23–25], providing symplectic tracking of protons with an integrated Monte-Carlo routine to simulate proton-matter interaction. SixTrack is based on symplectic tracking maps derived from the mono-nuclide accelerator Hamiltonian with $\chi = 1$ and $m = m_0$ for all particles [26–28]. The interaction of protons with the collimators is simulated by means of an integrated Monte-Carlo event generator which simulates scattering from MCS, energy loss from ionization and nuclear effects [17]. The tracks of particles scattered out of the collimators are compared to a detailed model of the LHC aperture to identify the loss location. Particles undergoing inelastic interactions in the collimator which are not single diffractive are

considered to be lost. The number N_p of lost protons per bin of $\Delta s = 10\,\text{cm}$ is normalized by number of particles lost in the LHC collimators N_{tot} to derive the local cleaning inefficiency $\eta(s)$

$$\eta(s) = \frac{N_p(s)}{\Delta s\, N_{\text{tot}}}\,. \tag{14}$$

Simulations of the heavy-ion collimation efficiency must take into account the different interactions of heavy-ions with the collimator materials, in particular by EMD and nuclear fragmentation processes. A suitable heavy-ion tracking software must take into account mass and charge of the out-scattered ion-fragments to accurately model dispersion. Hence, specialized software must be used for heavy-ion collimation simulations, requiring additional features compared to SixTrack. In this section an overview of the history of heavy-ion collimation simulation tools for LHC applications is given.

4.2 ICOSIM (2004)

In 2004, the simulation software Ion Collimation Simulation (ICOSIM) was developed to anticipate the heavy-ion collimation efficiency for the LHC [20, 29]. The simulation approach is based on several consecutive steps. In a first linear mapping, an initial sample of particles is tracked turn-by-turn at the primary collimator. Every 100 turns, random transverse kicks are applied to simulate diffusion. This initial tracking is performed until all ions of the initial sample have hit the primary collimator, to determine their impact coordinates. In the next step, the interaction of the ions with the collimator material is simulated using an integrated Monte-Carlo routine, based on tabulated fragmentation cross sections that are generated beforehand with the Monte-Carlo event generator FLUKA [18, 30, 31]. The particle-matter interaction neglects angular scattering from the fragmentation process and only keeps track of the heaviest fragment created in an interaction. The out-scattered ion fragments are then tracked through the LHC ring element by element using matrix multiplication including dispersion in linear approximation. The loss location of the ions is determined by comparing the particle positions with a simplified model of the magnet aperture.

The comparison of lossmaps simulated with ICOSIM to measured BLM data shows that the physics models used in ICOSIM are not detailed enough to accurately model heavy-ion losses from collimation (see [12]). This observation motivated the development of the new simulation tool STIER to overcome the limiting simplifications.

4.3 STIER (2014)

SixTrack with Ion-Equivalent Rigidities (STIER) was developed in 2014 to increase the agreement between measurement and simulations. It is based on proton tracking in SixTrack, using the approach presented in Section 3.2 tracking heavy-ions as protons of equivalent rigidity.

It is hence necessary to perform the particle-matter interaction simulation externally. Given the hierarchy of the LHC collimation system the dominating part of collimation losses can be simulated by considering only the interaction of the primary $^{208}\text{Pb}^{82+}$ beam with the primary collimator, which can be done e.g. with FLUKA. STIER simulations carried out so far used a three-stage simulation chain consisting of

1. An initial optics calculation with MAD-X to produce the SixTrack input and obtain the phase space parameters of the particles impacting the TCP. The latter are used to calculate the impact angle $x'_{l/r}$ on the left and right TCP jaw [32]

$$x'_{l/r} = \mp N_P\, \alpha_x \sqrt{\frac{\epsilon_x}{\beta_x}}\,, \tag{15}$$

where α_x, β_x are the Twiss parameters and ϵ_x is the geometric emittance.

2. The fragmentation of the heavy ions at the primary collimator is simulated by means of FLUKA. The collimator is modelled as a block of carbon and the coordinates and species of the out-scattered ion fragments are saved as output. In a post/pre-processing computation the ion-equivalent proton momenta are computed and saved together with the 4D position coordinates in an input file for SixTrack.
3. The data sampled with FLUKA represents the expected particle distribution of heavy-ion fragments after the passage of the TCP. Hence, the tracking simulation must be started at the TCP. The particle-matter interaction routine in SixTrack is specific to protons, such that it must be evaded in heavy-ion collimation simulations. However, the collimators must be included in the simulation, to identify heavy-ion losses at collimators. The SixTrack input is therefore modified to treat the collimators as perfect absorbers. The acceleration by the RF cavities is in reality dependent on the particle charge [22], so STIER can only provide 4D tracking of the heavy ions.

Evidently, STIER overestimates losses at collimators and subsequent interactions of fragments scattered out of the TCP are not modelled. However, heavy-ion loss maps simulated with STIER show a good agreement with measured data (see Section 5.1). Compared to its predecessors the predidictive power of STIER is significantly enhanced, mainly due to the inclusion of angular scattering and energy transfer from the fragmentation process [12]. The development of STIER was a major step in the theoretical understanding of heavy-ion losses at the LHC.

4.4 hiSixTrack (2016)

Simulations with STIER can deliver good predictions of the LHC cleaning performance but the applied simplifications restrict the spectrum of applications. Besides simulations of the cleaning performance, estimates on the deposited energy in the magnet coils are important for the operation of the LHC [33]. They can be obtained by detailed shower propagation simulations, typically carried out with FLUKA. The input for these simulations is the distribution of impacting ions on the collimators, which must be generated with a collimation simulation tool. STIER can not be used for this purpose because the ions are tracked as protons and the particle-matter interaction simulation requires the information on the particle species. Furthermore, particles scattered out of collimators subsequent to the TCP may contribute to the loss pattern, which can only be simulated by performing particle-matter interactions at all collimators. Therefore it is necessary to store information on the particle species in the tracking routine.To enable these functionalities, the software heavy-ion SixTrack (hiSixTrack) [22, 34] was implemented as a successor of STIER.

4.4.1 Tracking

hiSixTrack is based on SixTrack in which additional tracking arrays store mass and charge of the tracked ions have been implemented. The proton tracking maps were replaced by the multi-nuclide tracking maps presented in [4, 22]. The calculation of χ requires to define nucleon number, charge number and rest mass of the reference species. Thanks to the generic implementation, hiSixTrack is the first heavy-ion tracking tool allowing to simulate longitudinal particle dynamics and hence synchronous six-dimensional symplectic tracking of arbitrary particles.

The tracking routine of hiSixTrack was extensively tested to ensure their accuracy. In Fig. 5, heavy-ion tracks simulated with hiSixTrack and STIER are compared against each other. The tracks are calculated for different nuclides with $\delta = 0$ but $\chi \neq 1$ starting from IP1 in a LHC lattice matched to $^{208}\mathrm{Pb}^{82+}$. Similar comparisons were carried out also for other scenarios with different values of δ and χ (see [4]). In all studied cases a full numerical agreeement of the heavy-ion tracks was observed between hiSixTrack and STIER, even for a large number of tracked turns through the LHC ring. Both models hence simulate the 4D particle tracks with the same precision.

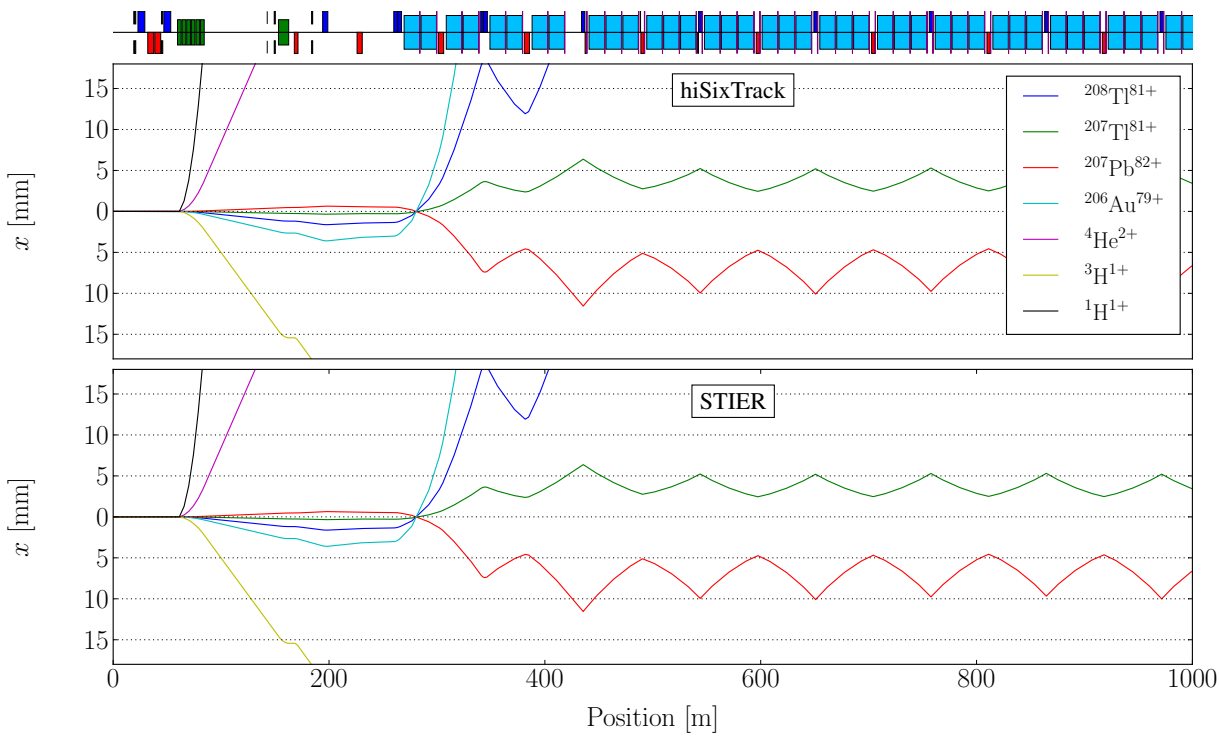

Fig. 5: Heavy-ion tracks for different on-momentum ($\delta = 0$) isotopes unmatched to the magnetic lattice ($\chi \neq 1$) starting with the same initial conditions in IP1, simulated with hiSixTrack (top) and STIER (bottom).

In addition to the features provided by STIER, the software hiSixTrack enables the possibility of six-dimensional tracking and on-line coupling to FLUKA (see next chapter). The generic implementation based on the multi-nuclide accelerator Hamiltonian is the most generic approach possible, enabling a high number of unprecedented applications. The generic tracking routine can be further extended to simulate other effects or tracking maps for other beam line elements, e.g. beam-beam interaction, crab cavities or electron lenses [21].

4.4.2 Coupling to FLUKA

The software hiSixTrack can be coupled to FLUKA, allowing the performance of FLUKA particle-matter interaction simulations at each of the collimators. The underlying framework for the so called hiSixTrack-FLUKA coupling [34] is the SixTrack-FLUKA coupling for the simulation of proton collimation [35]. Compared to the latter, the coupling of hiSixTrack to FLUKA requires the exchange of additional information, in particular the information on the species of the exchanged ion. The framework allows to simulate multiple interaction processes in the collimation system, which are impossible to take into account with the STIER approach, where the collimators must be treated as perfect absorbers.

4.4.3 Summary

The coupling between the tracking tool hiSixTrack and FLUKA combines two of the most sophicsticated simulation tools for their respective purpose to a powerful environment for the simulation of heavy-ion collimation and other applications. A comparison between simulated and measured loss maps is presented in the next section.

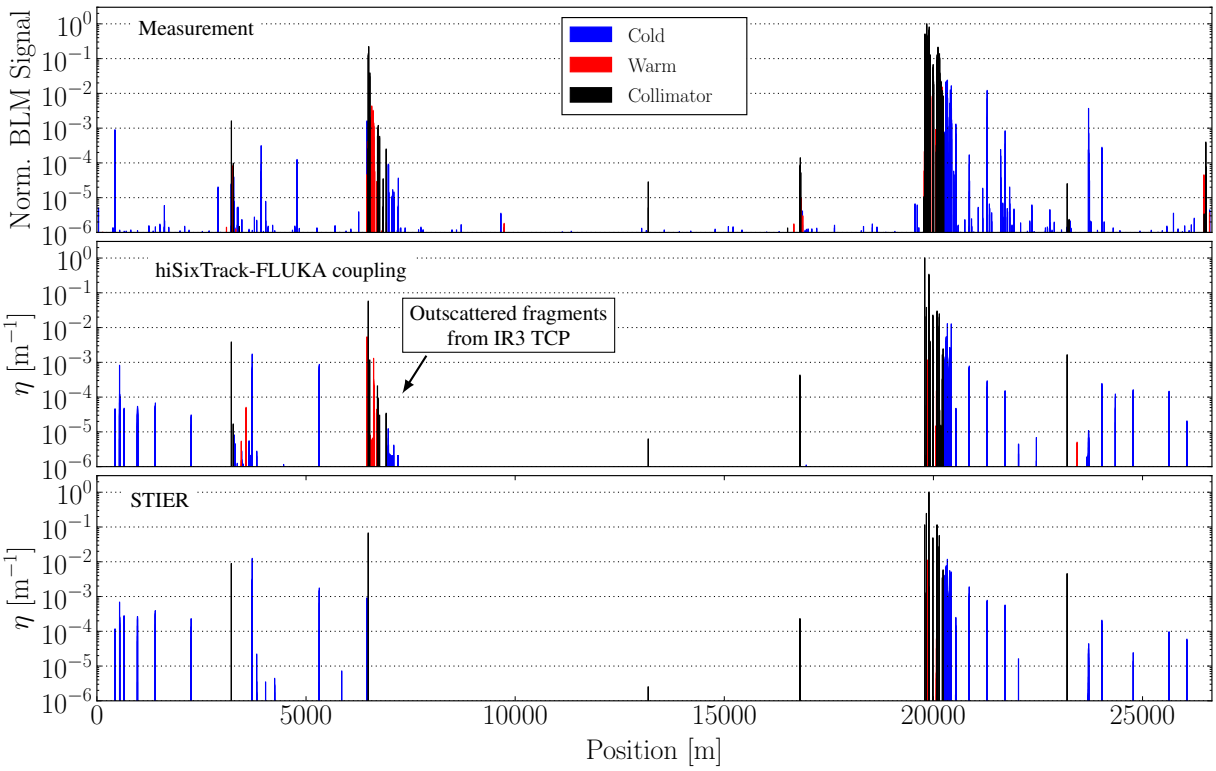

Fig. 6: B1H betatron loss maps measured in the 2011 heavy-ion run compared to simulations with the hiSixTrack-FLUKA coupling and STIER.

5 Applications

5.1 LHC Qualification Loss Maps

Simulated loss maps for heavy-in collimation are based on a more generic definition of the local cleaning inefficiency

$$\eta(s) = \frac{\sum_i E_i(s)}{\Delta s \, E_{\text{tot}}} \,, \tag{16}$$

where E_i is the energy if the ion i lost at the position s and E_{tot} is the total energy of all ions lost in the LHC collimators. This re-definition of the local cleaning inefficiency is necessary because the energy of ion fragments can vary significantly. The energy of a $^{208}\text{Pb}^{82+}$ ion scattered out of a LHC collimator is typically larger by two orders of magnitude compared to an outscattered proton. In addition, the energy per nucleon of the indiviual ions can vary significantly (see [4]), hence the local cleaning inefficiency is not correctly modelled by counting the number of impacting nucleons.

A comparison of measured and simulated loss maps is shown in Fig. 6 for the LHC in the configuration of the 2011 heavy-ion run at an energy of 3.5 Z TeV. The collimator and optics settings are summarized in [12]. It shall be pointed out that the measured BLM signal and the simulated local cleaning inefficiency should not be compared quantitatively. The measured BLM signal depends on an unknown repsonse function for upstream particle losses, while the simulated cleaning inefficiency is determined with a full and immediate detection of particle losses at the beam pipe.

Both simulation tools show a good agreement with the measured data. The losses in the superconducting regions downstream of IR7 are qualitatively well reproduced. A significant difference between the simulation codes is the modelling of the losses downstream of the momentum collimation region IR3. While these losses are not simulated in STIER, because of the absence of a multi-passage interaction model, they are visible in the simulation with the hiSixTrack-FLUKA coupling. This shows that the

inclusion of the interaction at all collimators does indeed change the loss pattern.

5.2 Mitigation of Losses in Operation

Collimation simulation tools play a crucial role in the understanding and potential mitigation of undesired losses in operation. This shall be illustrated on the example of the 2015 heavy-ion run with $^{208}Pb^{82+}$ ions.

In late 2015, the LHC was operated with $^{208}Pb^{82+}$ ion beams at an energy of 6.37 Z TeV [36]. During operation in collision, high losses at the horizontal tertiary collimator left of IR2 (TCT2) were measured (see top panel of Fig. 7). They reached amplitudes of 10^{-2} and induced undesired background to the ALICE experiment. From the affected TCT it was possible to conclude that the losses were caused by particles of beam 1 in the horizontal plane. To understand and potentially mitigate these losses, simulations with STIER were thoroughly analyzed [4].

The STIER simulations for B1H showed that the simulated loss signal at the TCT2 is significantly higher for particles scattered out of the left TCP jaw, than for those scattered out of the right jaw (see middle and bottom panel in Fig. 7). Instead of being lost at the TCT2, the particles starting from the right TCP jaw are lost in the momentum cleaning insertion IR3. The first conclusion to draw from the STIER simulation is that the losses observed in the IR2 TCT should be reduced if the left TCP jaw was retracted and all primary losses took place at the right TCP jaw.

The analysis of the loss composition at the TCT2 shows that 92.5% of the losses are caused by the isotope of the reference species $^{207}Pb^{82+}$ starting from the left jaw of the primary collimator (see Tab. 2). This isotope is created with a high abundance via EMD. Assuming that a realistic impact parameter was chosen for the FLUKA simulation (3μm in this study case), one can quantify the potential for loss reduction to be approximately one order of magnitude if the left TCP jaw was retracted.

The track of this nuclide simulated with STIER is shown in Fig. 8. It is clearly visible how the particle track is not intercepted by the secondary collimators. The horizontal TCT in IR8 (TCTH.4L8.B1, called TCT8 in the following) is passed by at a very short distance of less than 2 σ. The isotope ultimately impacts the TCTH.4L2.B1 after having moved through the LHC lattice for 10km. This result shows that it is essential to have a reliable and accurate tracking routine also for heavy-ions, because the ion fragments from IR7 can travel for long distances through the LHC.

The analysis of the particle track thus shows that, if the simulation is accurate, the secondary beam of $^{207}Pb^{82+}$ can be intercepted by the TCT in IR8. By estimating the beam sice and the simulated distance of the $^{207}Pb^{82+}$ track from the IR8 TCT, it is also possible to quantify the possible loss reduction as a function of the TCTH.4L8.B1 half gap. A detailed description is given in [4].

Both strategies of loss mitigation were tested with beam in the LHC, and the measured cleaning inefficiency at the TCT2 is illustrated in Fig. 9. In both tested scenarios the prediction made with STIER could be confirmed even quantitatively in LHC operation[1]. As expected, the measured BLM signal at

[1]Note that a quantitative comparison is only possible because the data is measured at the same BLM.

Table 2: Loss composition at the TCT2 simulated with STIER for B1H in the 2015 configuration using a TCP impact parameter of 2 μm. The energy fraction is calculated from the number of particles of each isotope, weighted with the particle momenta.

Isotope (A,Z)	TCP jaw	Fraction (%)
$^{207}Pb^{82+}$	left	92.5
$^{204}Tl^{81+}$	right	3.6
$^{202}Hg^{80+}$	left	2.2
$^{199}Au^{79+}$	right	0.3

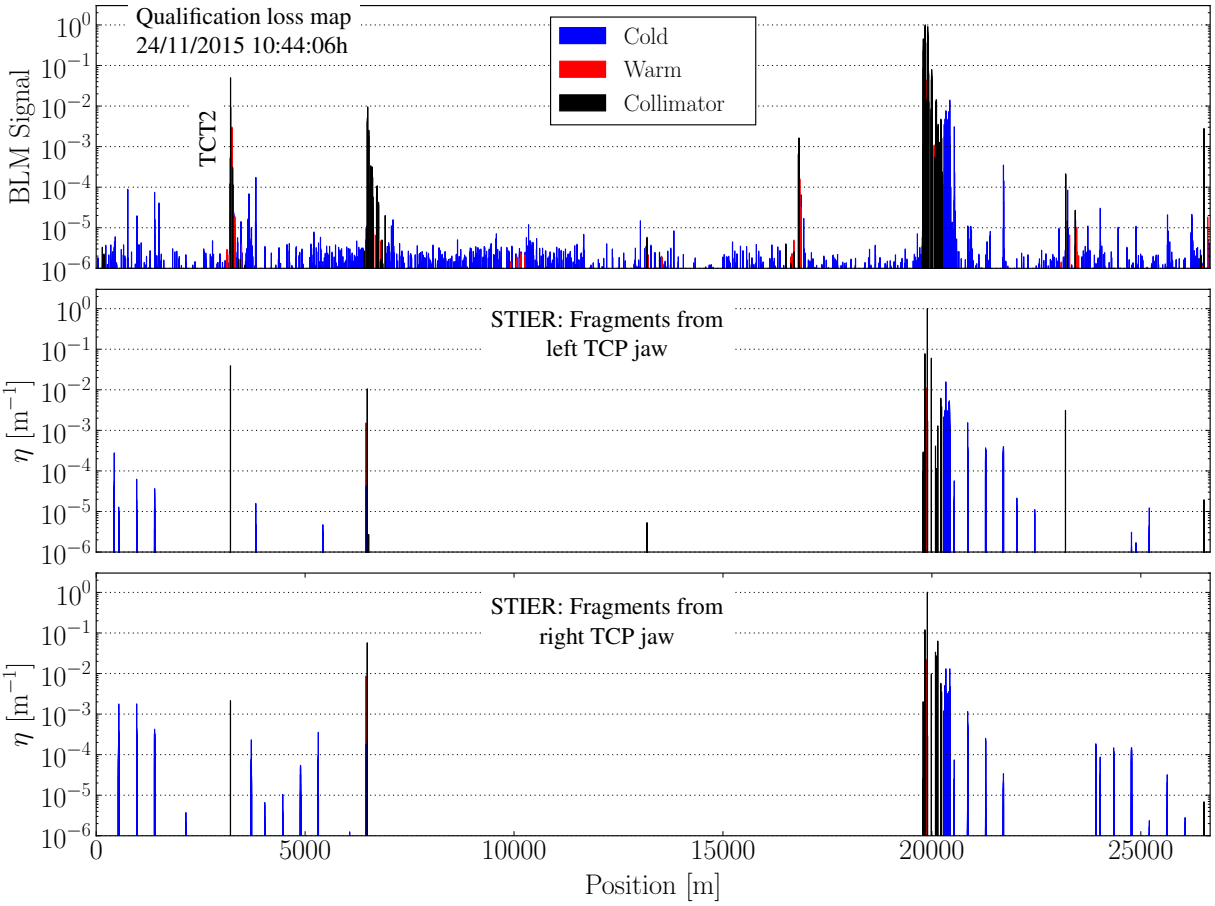

Fig. 7: Top panel: B1H qualification loss map measured in the 2015 heavy-ion run. Middle and bottom panel: STIER simulation result of the $^{208}Pb^{82+}$ cleaning inefficiency for B1H in the configuration of the 2015 heavy-ion run at 6.37 Z TeV. The simulation result is shown for particles starting at the left and at the right horizontal TCP jaw separately. Both simulations are carried out with 6×10^6 initial $^{208}Pb^{82+}$ particles.

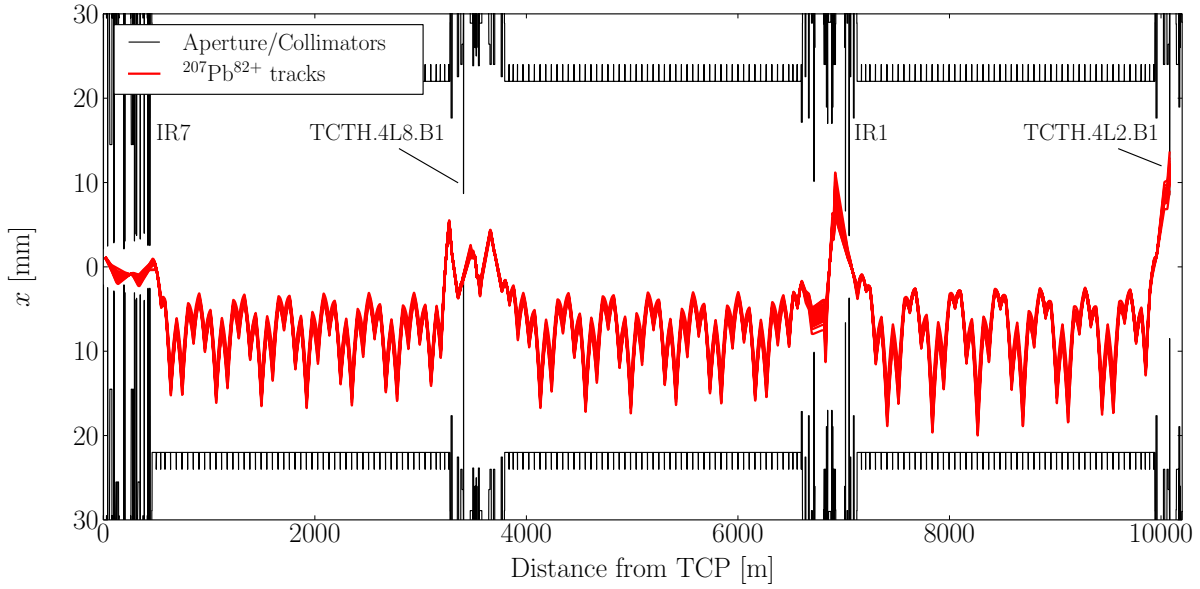

Fig. 8: Simulated track of the secondary $^{207}Pb^{82+}$ beam starting at the left jaw of the horizontal TCP in IR7, which is lost at the TCT2.

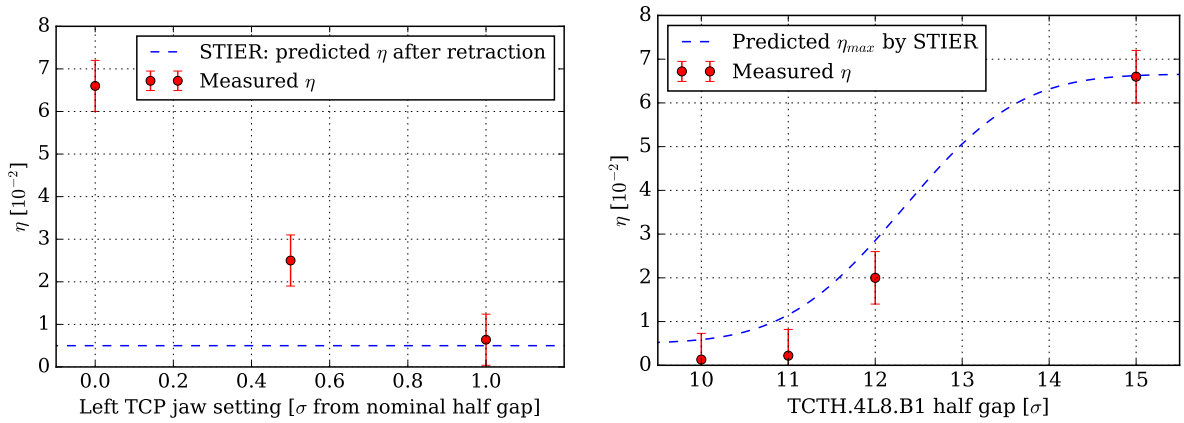

Fig. 9: Left: Measured loss signal at the TCT2 with different settings of the left TCP jaw. The blue dashed line shows the STIER prediction for a fully retracted jaw. Right: Measured loss signal at the TCT2 with different settings of the TCT8

the TCT2 is reduced by approximately one order of magnitude when the left TCP jaw is retracted. The measured TCT2 BLM signal with the different settings of the TCT8 is also in good agreement with the STIER prediction (note that in this case, the prediction refers to the maximum expectable signal for several reasons, see [4]).

In conclusion, the example illustrates how heavy-ion collimation simulations can be used to identify the origin of disturbing loss signals and to develop strategies to mitigate them. Although the 2015 collimator settings were not changed (e.g. non-symmetric TCP settings could have been applied), the knowledge of the loss origin could deliver essential input for the optimization of the collimation system. The experience gained was taken into account in the preparation of the 2016 heavy-ion run.

6 Summary and Outlook

Collimation simulation tools are crucial to provide safe operation uninterrupted by magnet quenches with both proton and heavy-ion beams. In this chapter we have outlined the requirements for heavy-ion collimation simulations, essentially consisting of a combination of reliable fragmentation simulations and accurate tracking tools modelling dispersion from mass and charge differences. It was shown how the heavy-ion tracking tools used for the LHC have evolved over more than a decade with improving the accuracy of the simulated loss maps.

The simulation tool STIER was introduced as a new development to improve the predictive power compared to its predecessor ICOSIM. The present state of the art simulation tool hiSixTrack is providing sophisticated physics models and can be used for a broad variety of applications. With its coupling to FLUKA it can be used to simulate the heavy-ion collimation efficiency with unprecedented accuracy.

The impact heavy-ion collimation simulations can have on the machine in operation was demonstrated for the example of the 2015 heavy-ion run. In this run, the STIER simulations could be used to understand heavy-ion loss patterns. The information was ultimately used to successfully manipulate the losses in the LHC. Such techniques may be crucial also in future heavy-ion operation.

Further analyses of energy deposition in LHC magnets have been carried out with FLUKA, using hiSixTrack simulation data as input [37]. This information will be used in the future to define BLM thresholds and estimate quench limits by combining simulations with experimental data.

References

[1] O. Brüning *et al.*, *LHC Design Report (Volume I, The LHC Main Ring)*, vol. CERN-2004-003-V-1. CERN, 2004.

[2] J. M. Jowett *et al.*, "The 2016 Proton-Nucleus Run of the LHC," *Proceedings of IPAC 2017, Kopenhagen, Denmark*, no. TUPVA014, 2017.

[3] G. Apollinari and others (eds), "High-Luminosity Large Hadron Collider (HL-LHC): Preliminary Design Report," *CERN Publication*, no. CERN-2015-005, 2015.

[4] P. D. Hermes, *Heavy-Ion Collimation at the Large Hadron Collider - Simulations and Measurements*. Doctoral thesis, Westfälische Wilhelms-Universität Münster, Germany, 2016.

[5] R. W. Assmann *et al.*, "The final collimation system for the LHC," *Proceedings of EPAC 2006, Edinburgh, Scotland*, no. TUODFI01, pp. 986–988, 2006.

[6] S. Redaelli, "The collimation system: defence against beam loss," *CERN Courier*, 2013.

[7] E. Holzer *et al.*, "Beam loss monitoring system for the LHC," *CERN-AB-2006-009 BI*, 2005.

[8] E. Holzer *et al.*, "Development, Production and Testing of 4500 Beam Loss Monitors," *Proceedings of EPAC 2008, Genoa, Italy*, no. TUPC037, p. 1134, 2008.

[9] R. Bruce *et al.*, "Measurements of heavy ion beam losses from collimation," *Phys. Rev. ST Accel. Beams*, vol. 12, no. 011001, 2009.

[10] R. Bruce *et al.*, "Simulations and measurements of beam loss patterns at the CERN Large Hadron Collider," *Phys. Rev. ST Accel. Beams*, vol. 17, no. 081004, 2014.

[11] P. D. Hermes *et al.*, "Studies on Heavy Ion Losses from Collimation Cleaning at the LHC," *Proceedings of HB 2014, East-Lansing, MI, USA*, no. MOPAB43, pp. 138–142, 2014.

[12] P. D. Hermes *et al.*, "Measured and Simulated Heavy-Ion Beam Loss Patterns at the CERN Large Hadron Collider," *Nucl. Instr. Meth. Phys. Res. A*, vol. 819, pp. 73–83, 2016.

[13] P. D. Hermes *et al.*, "LHC Heavy-Ion Collimation Quench Test at 6.37 Z GeV," vol. CERN-ACC-NOTE-2016-0031 MD, 2016.

[14] J. Beringer *et al.*, "Review of Particle Physics," *Phys.Rev.*, vol. D86, p. 010001, 2012.

[15] H. H. Braun *et al.*, "Hadronic and electromagnetic fragmentation of ultrarelativistic heavy ions at LHC," *Phys. Rev. ST Accel. Beams*, vol. 17, p. 021006, 2014.

[16] J. Bartke, *Relativistic Heavy Ion Physics*. World Scientific Publishing, 2009.

[17] C. Tambasco, "An improved scattering routine for collimation tracking studies at LHC," Master's thesis, 2014. CERN-THESIS-2014-014.

[18] A. Fassò *et al.*, "The physics models of FLUKA: status and recent developments," *Proceedings of CHEP 2003, La Jolla, California, USA*, no. MOMT005, 2003.

[19] B. V. Carlson *et al.*, "Fermi breakup and the statistical multifragmentation model," *Nuclear Physics A*, vol. 876, pp. 77 – 92, 2012.

[20] H. H. Braun *et al.*, "Collimation of heavy ion beams in LHC," *Proceedings of EPAC 2004, Lucerne, Switzerland*, no. MOPLT010, p. 551, 2004.

[21] R. De Maria, M. Fitterer, and M. Fjellstrom, "SixTrackLib Manual," 2015.

[22] P. D. Hermes, R. Bruce, and R. De Maria, "Symplectic Tracking of Multi-Isotopic Heavy-Ion Beams in SixTrack," *Proceedings of IPAC 2016, Busan, Korea*, no. TUPMW015, pp. 1450–1453, 2016.

[23] F. Schmidt, "SixTrack Version 4.2.16 Single Particle Tracking Code Treating Transverse Motion with Synchrotron Oscillations in a Symplectic Manner - User's Reference Manual," 1994. CERN/SL/94-56 (AP).

[24] T. Trenkler and J. Jeanneret, "K2: A Software Package evaluating Collimation Systems in Circular Colliders (Manual)," *CERN SL Note, SL/Note 94-105 (AP)*, 1994.

[25] G. Robert-Demolaize *et al.*, "A new Version of SixTrack with Collimation and Aperture Interface," *Proceedings of PAC 2005, Knoxville, Tennessee, USA*, no. FPAT081, p. 4084, 2005.

[26] D. P. Barber, G. Ripken, and F. Schmidt, "A non-linear canonical formalism for the coupled synchro-betatron motion of protons with arbitrary energy," vol. DESY-87-036, 1987.

[27] K. Heinemann, G. Ripken, and F. Schmidt, "Construction of Nonlinear Symplectic Six-Dimensional Thin-Lens Maps by Exponentiation," vol. DESY-95-189, 1995.

[28] G. Ripken and F. Schmidt, "A symplectic Six-Dimensional Thin-Lens Formalism for Tracking," vol. CERN-SL-95-12 (AP), 1995.

[29] N. Holden, "Development of the ICOSIM Program and Application to Magnetised Collimators in the LHC," Tech. Rep. CERN-AB-Note-2008-054, 2008.

[30] A. Ferrari, P. R. Sala, A. Fasso, and J. Ranft, "FLUKA: A multi-particle transport code (Program version 2005)," *CERN-2005-10 (2005), INFN/TC_05/11, SLAC-R-773* , 2005.

[31] T. T. Böhlen *et al.*, "The FLUKA code: developments and challenges for high energy and medical applications," *Nuclear Data Sheets*, vol. 120, pp. 211–214, 2014.

[32] H. Wiedemann, *Particle accelerator physics I: basic principles and linear beam dynamics*, vol. 1. Springer Verlag, 1999.

[33] E. Skordis *et al.*, "Impact of Beam Losses in the LHC Collimation Regions," *Proceedings of IPAC 2015, Richmond, VA, USA*, no. TUPTY046, pp. 2116–2119, 2015.

[34] P. D. Hermes *et al.*, "Simulation of Heavy-Ion Beam Losses with the SixTrack-FLUKA Active Coupling," *Proceedings of IPAC 2016, Busan, Korea*, no. WEPMW029, pp. 2490–2493, 2016.

[35] A. Mereghetti *et al.*, "SixTrack-FLUKA active coupling for the upgrade of the SPS Scrapers," *Proceedings of IPAC 2013, Shanghai, China*, no. WEPEA064, pp. 2657–2659, 2013.

[36] J. M. Jowett *et al.*, "The 2015 Heavy-Ion Run of the LHC," *Proceedings of IPAC 2016, Busan, Korea*, no. TUPMW027, pp. 1493–1496, 2016.

[37] E. Skordis *et al.*, "Study of the 2015 Top Energy LHC Collimation Quench Tests through and advanced Simulation Chain," *Proceedings of IPAC 2017, Kopenhagen, Denmark*, no. MOPAB012, 2017.